SCALING BEHAVIOR OF CIRCULAR COLLIDERS DOMINATED BY SYNCHROTRON RADIATION

Richard Talman*
Laboratory of Elementary-Particle Physics Cornell University
***richard.talman@cornell.edu**

White Paper at the 2015 IAS Program on the Future of High Energy Physics

TUTORIAL LECTURE I

This file contains the material presented in Lecture I. It mainly consists of pages extracted from the full paper, which has the title given above, with less important sections deleted and more important material underlined.

Abstract

Optimizing a facility having an electron-positron Higgs factory, followed decades later by a p,p collider in the same tunnel, is a formidable task. The CepC design study constitutes an initial "constrained parameter" collider design.

A scaling law formulation is intended to contribute to "ground-up" stage in the design of future circular colliders.

Equally important, by solving the lattice matching equations in closed form, as contrasted with running computer programs such as MAD, one can obtain better intuition concerning the fundamental parametric dependencies.

This paper concentrates primarily on establishing scaling laws that are fully accurate for a Higgs factory such as CepC. Dominating everything is the synchrotron radiation formula

$$\Delta E \propto \frac{E^4}{R}, \tag{1}$$

relating energy loss per turn ΔE, particle energy E and bend radius R. [2] This is the main formula governing tunnel circumference for CepC because increasing R decreases ΔE.

The same formula will possibly dominate future proton colliders as well.

CONTENTS

CONTENTS

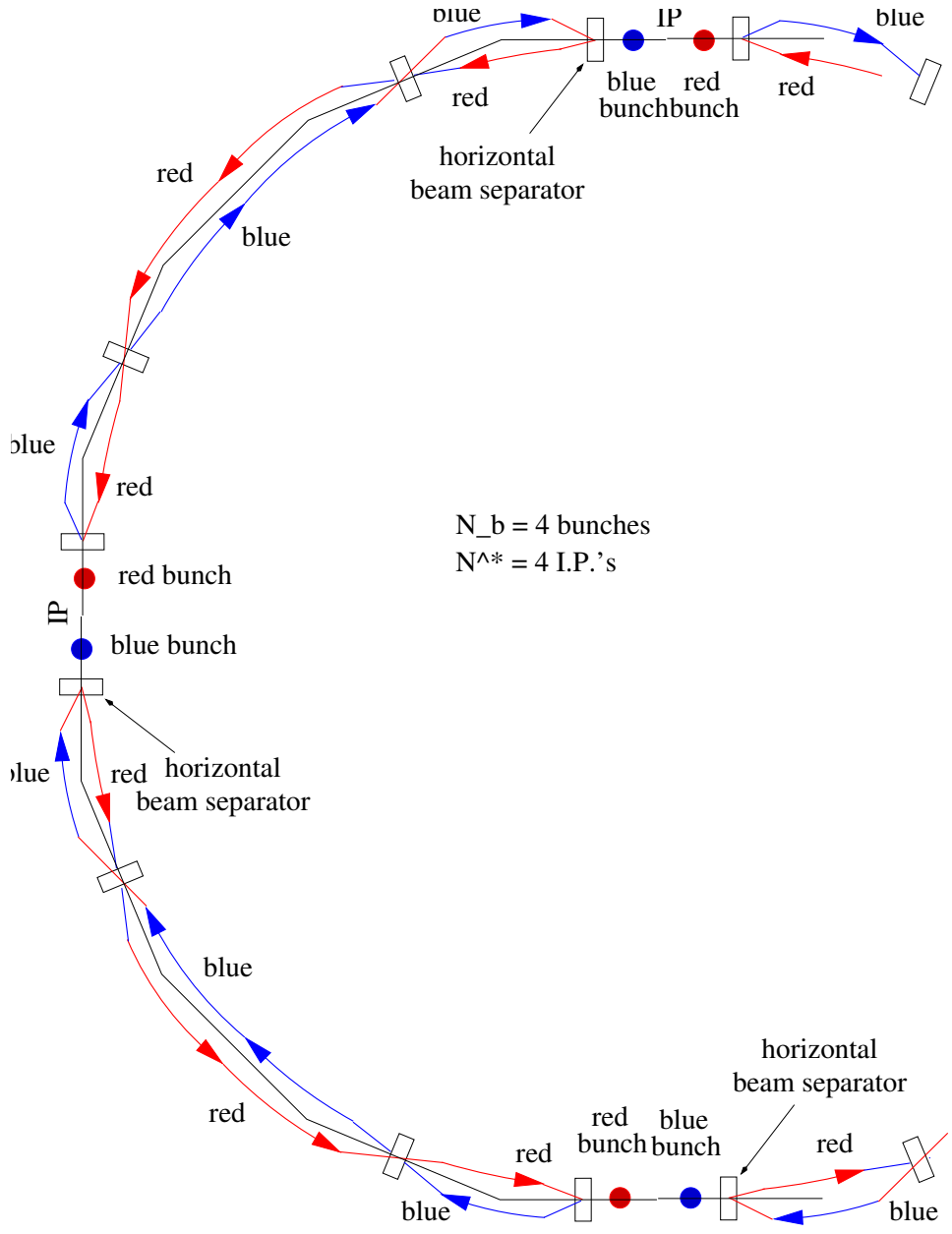

Figure: Schematic partial view of Higgs factory. As shown there are $N_b = 4$ bunches colliding at $N^* = 4$ collision points.

Unlike the Z_0, there is no unique "Higgs Factory energy". Rather there is the threshold turn-on of the cross section.

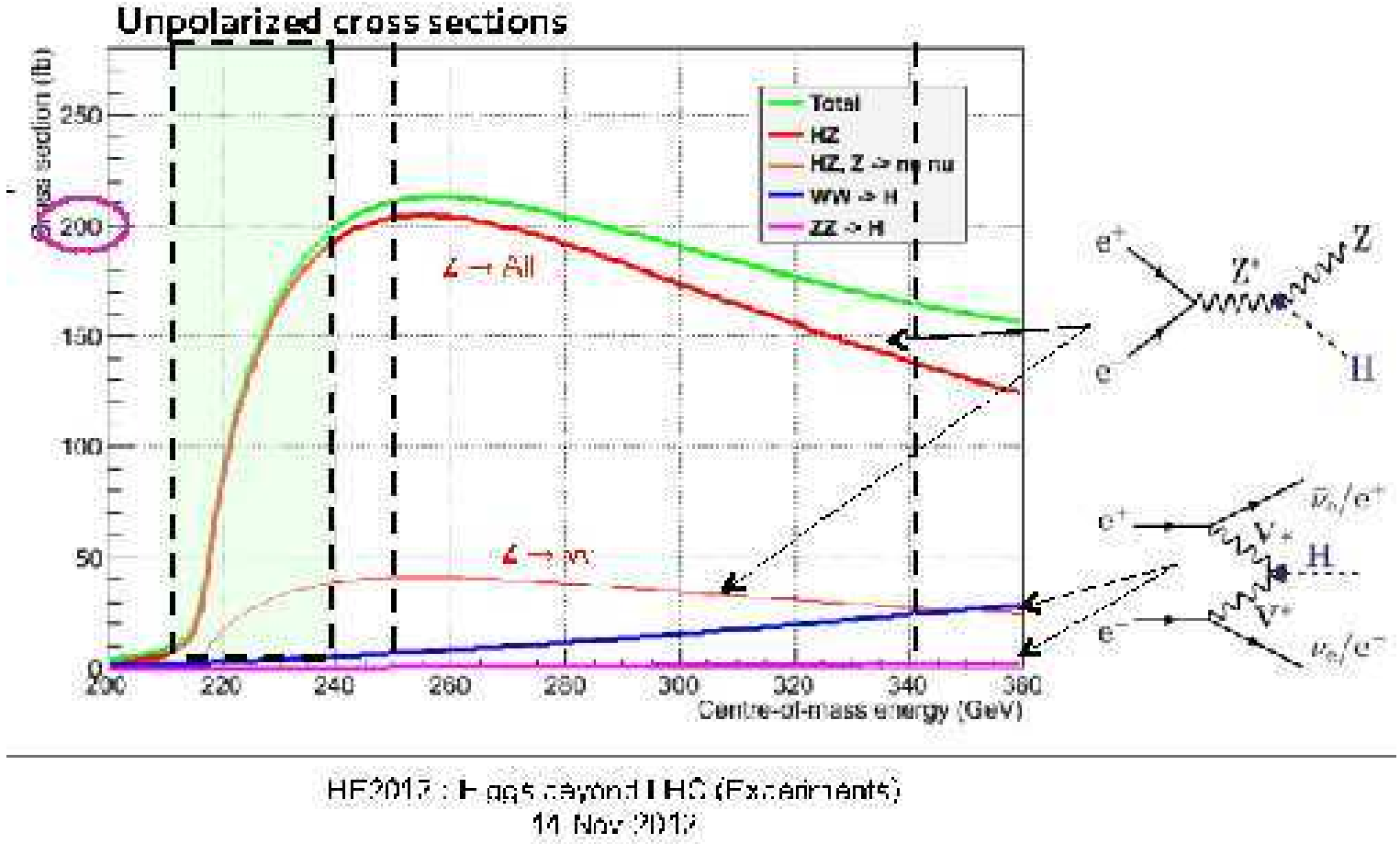

Figure: Higgs particle cross sections up to $\sqrt{s} = 0.3\,\text{TeV}$ (copied from Patrick Janot).

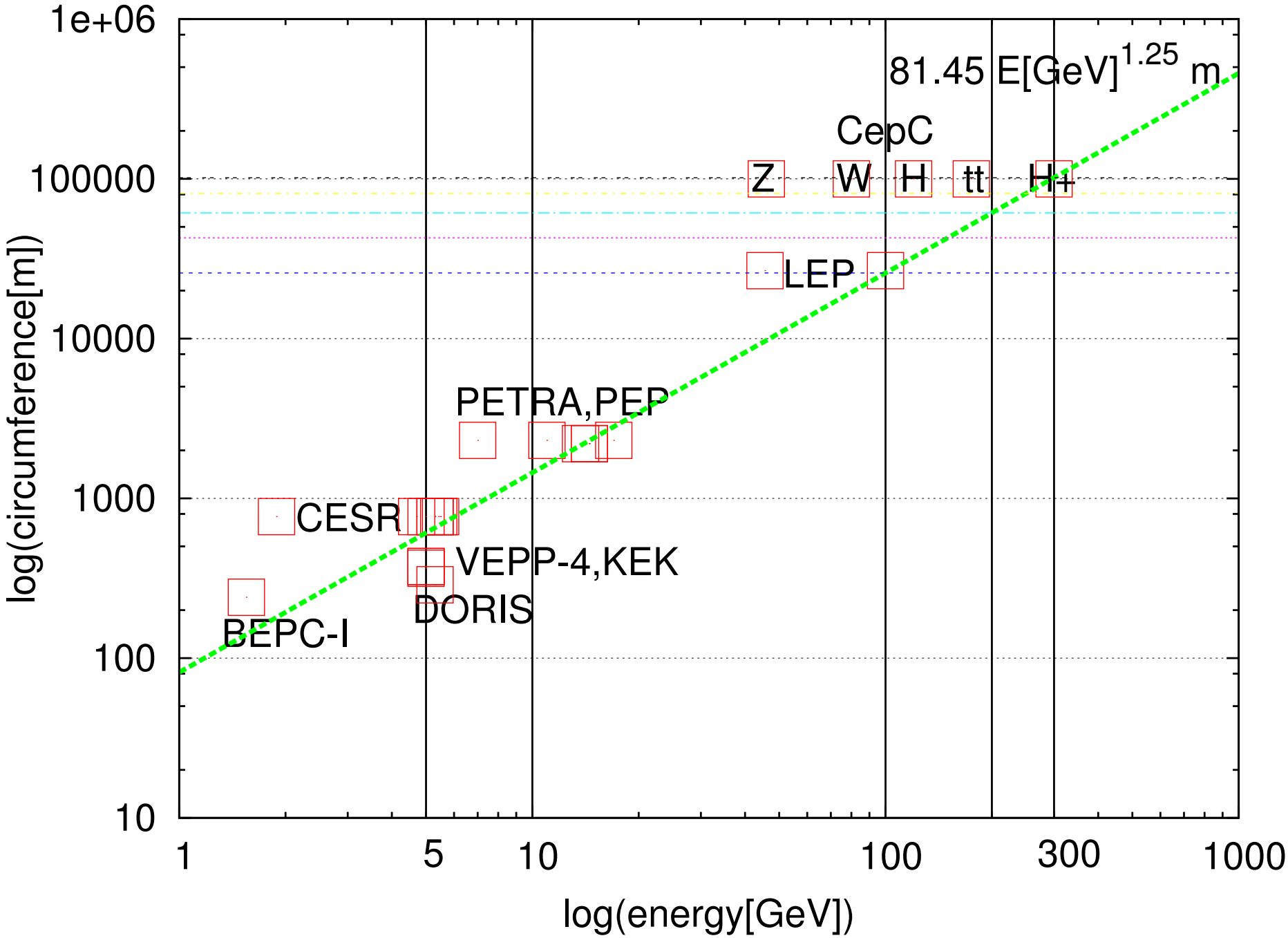
1e+06
100000
10000
1000
100
10
log(circumference[m])
1
5
10
100
300
1000
log(energy[GeV])
81.45 E[GeV]^1.25 m
CepC
Z
W
H
tt
H+
LEP
PETRA,PEP
CESR
VEPP-4,KEK
DORIS
BEPC-I

2.2 *Scaling up from LEP to Higgs Factory*

Radius Power Scale Invariant.

Higgs production was just barely beyond the reach of LEP's top energy, by the ratio 125 GeV/105 GeV = 1.19. **This should make the extrapolation from LEP to Higgs factory quite reliable. In such an extrapolation it is increased radius more than increased beam energy that is mainly required.**

One can note that, for a ring three times the size of LEP, the ratio of E^4/R (synchrotron energy loss per turn) is $1.19^4/3 = 0.67$—i.e. *less than final LEP operation*. Also, for a given RF power $P_{\rm rf}$, **the maximum total number of stored particles is proportional to R^2—doubling the ring radius cuts in half the energy loss per turn and doubles the time interval over which the loss occurs.** Expressed as a scaling law

$$\boxed{n_1 = \text{number of stored electrons per MW } \propto R^2.} \quad (3)$$

This is boxed to emphasize its fundamental importance. Following directly from Eq. (1), it is the main consideration favoring large circumference for both electron and radiation-dominated proton colliders.

These comments should completely debunk a long-held perception that LEP had the highest energy practical for an electron storage ring.

There are three distinct upper limit constraints on the luminosity.

maximum luminosity results when the ring parameters have been optimized so the three constraints yield the same upper limit for the luminosity. For now we concentrate on just the simplest luminosity constraint $\mathcal{L}^{\rm RF}_{\rm pow}$, the maximum luminosity for given RF power $P_{\rm rf}$. With n_1 being the number of stored particles per MW; f the revolution frequency; N_b the number of bunches, which is proportional to R; σ^*_y the beam height at the collision point; and aspect ratio σ^*_x/σ^*_y fixed (at a large value such as 15);

$$\mathcal{L}^{\rm RF}_{\rm pow} \propto \frac{f}{N_b}\left(\frac{n_1 P_{\rm rf}[\rm MW]}{\sigma^*_y}\right)^2. \quad (4)$$

Consider variations for which

$$P_{\rm rf} \propto \frac{1}{R}. \quad (5)$$

Dropping "constant" factors, the dependencies on R are, $N_b \propto R$, $f \propto 1/R$, and $n_1 \propto R^2$. With the $P_{\rm rf} \propto 1/R$ scaling of Eq. (5), $\mathcal{L}$ is independent of R. In other words, the luminosity depends on R and $P_{\rm rf}$ only through their product $RP_{\rm rf}$. Note though, that this scaling relation *does not* imply that $\mathcal{L} \propto P^2_{\rm rf}$ at fixed R; rather $\mathcal{L} \propto P_{\rm rf}$.

In this paper this scaling law will be used in the form

$$\boxed{\mathcal{L}(R, P_{\rm rf}) = f(RP_{\rm rf}),} \quad (6)$$

the luminosity depends on R and $P_{\rm rf}$ as a function $f(RP_{\rm rf})$ of only their product.

```
This assumes the arcs are "benign";
their influence independent of R.
```

Parameter Scaling with Radius. For simplicity, even if it is not necessarily optimal, let us assume the Higgs factory arc optics can be scaled directly from LEP values, which are: phase advance per cell $\mu_x = \pi/2$, full cell length $L_c = 79$ m.

Constant dispersion scaling formulas are given in Table 3. These formulas are derived in Section 4.2 "Lattice Optimization for Top-Off Injection". They are then applied to extrapolate from LEP to find the lattice parameters for Higgs factories of (approximate) circumference 50 km and 100 km, shown in Table 5.

```
<-- RF power
    beam-beam tune shift
    beamstrahlung
```

constant dispersion scaling

Parameter	Symbol	Proportionality	Scaling
phase advance per cell	μ		1
collider cell length	L_c		$R^{1/2}$
bend angle per cell	ϕ	$= L_c/R$	$R^{-1/2}$
quad strength $(1/f)$	q	$1/L_c$	$R^{-1/2}$
dispersion	D	ϕL_c	1
beta	β	L_c	$R^{1/2}$
tunes	Q_x, Q_y	R/β	$R^{1/2}$
Sands's "curly H"	$\mathcal{H}$	$= D^2/\beta$	$R^{-1/2}$
partition numbers	$J_x/J_y/J_\epsilon$	$= 1/1/2$	1
horizontal emittance	ϵ_x	$\mathcal{H}/(J_x R)$	$R^{-3/2}$
fract. momentum spread	σ_δ	$\sqrt{B}$	$R^{-1/2}$
arc beam width-betatron	$\sigma_{x,\beta}$	$\sqrt{\beta\epsilon_x}$	$R^{-1/2}$
-synchrotron	$\sigma_{x,synch.}$	$D\sigma_\delta$	$R^{-1/2}$
sextupole strength	S	q/D	$R^{-1/2}$
dynamic aperture	$x^{\max}$	q/S	1
relative dyn. aperture	$x^{\max}/\sigma_x$		$R^{1/2}$
pretzel amplitude	x_p	σ_x	$R^{-1/2}$

Parameter	Symbol	Value	Unit	Energy-scaled	Radius-	scaled
bend radius	R	**3026**	m	**3026**	**5675**	**11350**
	$R/3026$			1	1.875	3.751
Beam Energy	E	**45.6**/91.5	GeV	**120**	**120**	**120**
Circumference	C	26.66	km	26.66	50	100
Cell length	L_c		m	79	108	153
Momentum compaction	α_c	1.85e-4		1.85e-4	0.99e-4	0.49e-4
Tunes	Q_x	90.26		90.26	123.26	174.26
	Q_y	76.19		76.19	104.19	147.19
Partition numbers	$J_x/J_y/J_\epsilon$	1/1/2		1/1.6/1.4 !	1/1/2	1/1/2
Main bend field	B_0	0.05/0.101	T	0.1316	0.0702	0.0351
Energy loss per turn	U_0	0.134/2.05	GeV	6.49	3.46	1.73
Radial damping time	τ_x	0.06/0.005	s	0.0033	0.0061	0.0124
	τ_x/T_0	679/56	turns	37	69	139
Fractional energy spread	σ_δ	0.946e-3/1.72e-3		0.0025	0.0018	0.0013
Emittances (no BB), x	ϵ_x	22.5/30	nm	21.1	8.2	2.9
y	ϵ_y	0.29/0.26	nm	1.0	0.4	0.14
Max. arc beta functs	$\beta_x^{\max}$	125	m	125	171	242
Max. arc dispersion	$D^{\max}$	0.5	m	0.5	0.5	0.5
Beta functions at IP	β_x^*, β_y^*	2.0,0.05	m	1.25/0.04	N/Sc.	N/Sc.
Beam sizes at IP	σ_x^*, σ_y^*	211, 3.8	μm	178/11	N/Sc.	N/Sc.
Beam-beam parameters	ξ_x, ξ_y	0.037,0.042		0.06/0.083	N/Sc.	N/Sc.
Number of bunches	N_b	8		4	N/Sc.	N/Sc.
Luminosity	$\mathcal{L}$	2e31	$\mathrm{cm}^{-2}\mathrm{s}^{-1}$	1.0e32	N/Sc.	N/Sc.
Peak RF voltage	V_{RF}	380	MV	3500	N/Sc.	N/Sc.
Synchrotron tune	Q_s	0.085/0.107		0.15	N/Sc.	N/Sc.
Low curr. bunch length	σ_z	0.88	cm	$\frac{\alpha_c R \sigma_e}{Q_s E}$	N/Sc.	N/Sc.

Table 5: Higgs factory parameter values for 50 km and 100 km options. The entries are mainly extrapolated from Jowett's, 45.6 Gev report [8], and educated guesses. "N/Sc." indicates (important) parameters too complicated to be estimated by scaling. Duplicate entries in the third column, such as 45.6/91.5 are from Jowett [8]; subsequent scalings are based on the 45.6 Gev values.

12 F. ACCELERATOR FORMALISM

12.1 Introduction

This appendix is not really part of the paper. It is attached only for convenience in introducing elementar ac-

Optical lines are constructed from lenses, mirrors and free space. Charged particles lines are constructed from analogous magnets and field-free regions. For this reason the most fundamental features (Liouville's theorem and its generalizations, linear/nonlinear distinction, intensities, emittances, adiabatic invariance, and so on) apply equally to

```
eectrons, protons (even photons)
```

This chapter analyses the paraxial (i.e. nearly parallel) propagation of particles, be they electrons or `protons`

12.2 Coordinate definitions

By definition, a beam is a number (usually billions and billions) of particles all traveling more or less parallel. For purposes of description it is useful to start by picking some "most-central" particle as a "reference particle" and describing its "ideal" or "reference" ray or trajectory through the system. Typically this ray passes through the centers of all the optical elements making up the beam line. Any particular point on the reference trajectory can be located by global Cartesian coordinates (X,Y,Z) relative to some fixed origin. But, to take advantage of the essentially one dimensional placement of elements it is profitable to locate elements by arc length (called s) from the origin along the central ray. Once these coordinates are known for the central particle, all the other particles in the beam can be located by relative coordinates. For these relative coordinates it is convenient to use a reference frame aligned with the central ray. "Tangential" or "longitudinal" displacements are specified by incremental arc length $z = \Delta s$ and (x,y) serve as "transverse" coordinates, with x usually being horizontal and y vertical. The longitudinal coordinates s and z increment trivially in drift[9] regions—by simple addition. For relativistic particles, s is proportional to t ($s = vt$, $v \approx c$) and s can take over from t the role of "independent variable".[10]

There is nothing "small" about the reference trajectory—in a storage ring it bends through 2π, in a light beam it may reflect through comparably large angles. On the other hand there is much that is "small" about the motion of particles relative to the reference particle and, of course, that is why local coordinates are introduced. Loosely speaking then, the coordinates (X,Y,Z,s) are "large" and the coordinates (x,y,z) are "small". The fundamental beam properties mentioned in the first paragraph apply primarily to these small displacements.

Much the same comments apply to velocity and momentum. The momentum components of the central ray are $(0,0,P_0)$ and, in the absence of accelerating elements, P_0 is constant. The momentum components of a beam particle are customarily expressed fractionally as the ratios[11]

$$(p_x, p_y, \delta) = \left(\frac{P_x}{P_0}, \frac{P_y}{P_0}, \frac{P - P_0}{P_0}\right), \qquad (145)$$

where $\delta = \Delta P/P_0 = (P - P_0)/P_0$ is therefore the fractional momentum deviation from the central momentum.

Far more fundamental is "Gaussian" (also known as "paraxial") optics, which describes transport systems in which the trajectory deviations, both displacement and slope, away from the reference trajectory are small enough to be treated by "linearized" equations of motion. That is, the differential equations governing the evolution of

$(x(s), y(s), \dots)$ are linear in $(x, y, \dots)$. Since these linearized equations are usefully expressed using matrices, such optical systems are said to be satisfy "matrix optics". The fundamental characteristics listed in the first paragraph are most easily described in terms of these matrices, and the "linear" distinction listed there is synonymous with "paraxial".

The propagation of a beam of particles through a sequence of beam line elements can be viewed from three different perspectives. These *particle*, *beam*, and *beam line* views will be taken up, in order, in the following sections

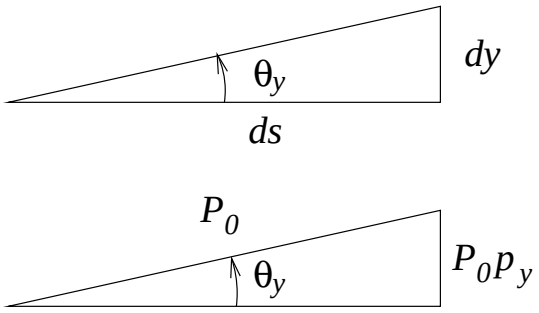

Figure 29: Relations among transverse angle, momentum, and slope.

12.3 1D transverse evolution equation

of description we therefore discuss now only a beam traveling along a straight channel centered on the s-axis, planning later to incorporate the (small) effects due to magnetic bending.

To prevent the eventual departure of even slightly divergent rays, it is necessary to have focusing elements such as quadrupoles for charged particles, fiber optics or optical lenses for visible photons, curved mirrors for x-rays, and so on. The differential equation describing such focusing is[12]

$$\boxed{\frac{d^2y}{ds^2} = K(s)y.} \qquad (146)$$

This equation will be referred to as the "focusing equation" adn $K(s)$ as the "vertical focusing strength". Just about everything of consequence in this chapter, and much of the next one, follows directly from this equation. The sign of K is like that of a Hooke's law force, negative for "restoring". The dependence of $K(s)$ on s permits the description of systems in which the focusing strength varies along the orbit. In particular, $K(s) \equiv 0$ describes "drift spaces" in which case Eq. (146) is trivially solved, and yields the obvious result that particles in free space travel in straight lines.

There are three candidates for describing particle directions: angle θ_y, slope y', or momentum p_y. All of these are exhibited in Fig. 29, and one sees that

$$y' \equiv \frac{dy}{ds} = \tan\theta_y = \frac{p_y}{\cos\theta_y}. \qquad (148)$$

This multiple ambiguity in what constitutes the coordinate conjugate to y is something of a nuisance at large amplitudes but, fortunately, all three definitions approach equality in the small-angle limit that characterizes Gaussian optics. One knows from Hamiltonian mechanics that p_y is the coordinate of choice but, while limiting ourselves to Gaussian optics, we will refer loosely to y' as "vertical momentum" so that we can refer to the (y, y')-plane as "vertical phase space".

<---remember this Eq.

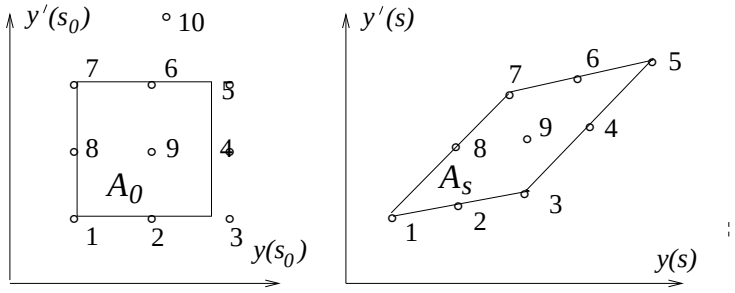

Figure 30: Phase space evolution of ten typical particles in advancing from s_0 to s along the beam line.

This can be expressed in matrix form, with $\mathbf{y} = (y, y')^{\mathrm{T}}$ being a "vector in phase space":

$$\begin{aligned}\mathbf{y}(s) &\equiv \begin{pmatrix} y(s) \\ y'(s) \end{pmatrix} \\ &= \begin{pmatrix} C(s,s_0) & S(s,s_0) \\ C'(s,s_0) & S'(s,s_0) \end{pmatrix} \mathbf{y}(s_0) \\ &= \mathbf{M}(s_0,s)\mathbf{y}(s_0). \end{aligned} \tag{151}$$

$$J(s_0,s) = \det \begin{vmatrix} \frac{\partial y}{\partial y_0} & \frac{\partial y}{\partial y'_0} \\ \frac{\partial y'}{\partial y_0} & \frac{\partial y'}{\partial y'_0} \end{vmatrix}. \tag{152}$$

From Eq. (151), suppressing the s_0-dependence, it can then be seen that

$$J(s) = \det |\mathbf{M}(s)| = C(s)S'(s) - S(s)C'(s) = 1. \tag{153}$$

which, being the Wronskian for the solutions $C(s)$ and $S(s)$, is known to be constant; that the value of the constant is 1 comes from evaluating $J(s_0)$, using Eqs. (149).

Particle trajectories in phase space cannot cross—this follows from the fact that instantaneous position and slope uniquely determine the subsequent motion. Hence the boundary will continue to be defined by particles 1 through 8 and a particle like 9 that is inside the box at s_0 will remain inside the box at s. Similarly, a particle like 10 will remain outside.

that the particle density $\rho(s)$ is, in fact, independent of s. This is Liouville's theorem, a result that can be discussed with various degrees of erudition and generality. But it is surprisingly simple in the present context. It is most succinctly stated by the requirement

$$\det |\mathbf{M}(s)| = 1, \tag{154}$$

which is the so-called "symplectic condition" in this special case of one dimensional motion.

12.4 Transfer matrices for simple elements

Drift space. The most important transfer matrix is $\mathbf{M}_l$, which describes propagation through a drift space of length ℓ. Since the orbits are given by $y(s) = y_0 + y'_0 s, y'(s) = y'_0$, we have

$$\mathbf{M}_l = \begin{pmatrix} 1 & \ell \\ 0 & 1 \end{pmatrix} \tag{155}$$

In the context of this book, the basis for calling drifts "the most important element" is that the synchrotron light beam line leading from storage ring to detection apparatus is one long drift section.

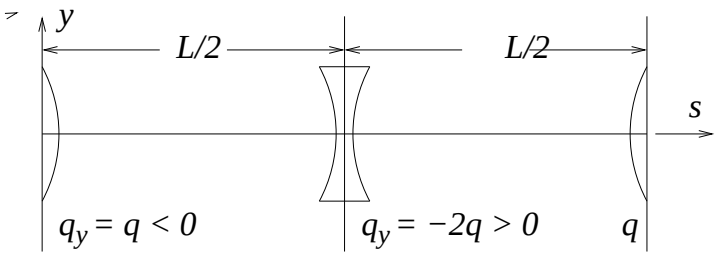

Figure 33: A standard "FODO cell" of length L, beginning and ending at the centers of (horizontally) thin focusing half-quads.

The "focal length" f of the lens, defined in Fig. 32, and the "lens strength" $q = -1/f$, are then given by[14]

$$q = -\frac{1}{f} = \frac{\Delta y'}{y} = K\Delta s. \tag{157}$$

Building in the (thin lens) approximation that y is contant through the lens, the transfer matrix is then given by

$$\mathbf{M}_q = \begin{pmatrix} 1 & 0 \\ q & 1 \end{pmatrix}. \tag{158}$$

As drawn in Fig. 32, K and q are positive, f is negative, and the lens is "defocusing".

recast as the deflection caused by an ideal lens of strength[15]

$$q_y = \frac{\Delta y'}{y} = K_y \Delta s, \quad \text{where} \quad K_y = \frac{c(\partial B_x/\partial y)}{(P_0 c/e)}. \quad (161)$$

Because of the Maxwell equation $\partial B_x/\partial y = \partial B_y/\partial x$, this vertical focusing strength is necessarily accompanied by horizontal focusing strength of opposite sign:[16]

$$q_x = -q_y. \quad (162)$$

To express this constraint succinctly it is convenient to write a 4×4 transfer matrix:

$$\mathbf{M}_q = \begin{pmatrix} 1 & 0 & 0 & 0 \\ -q & 1 & 0 & 0 \\ 0 & 0 & 1 & 0 \\ 0 & 0 & q & 1 \end{pmatrix}, \quad (163)$$

which acts on the vector $(x, x'y, y')^T$. (Unlike this, a visible light lens can have same sign off-diagonal terms—for example both focusing. Clearly this simplifies the design of lines for visible light.)

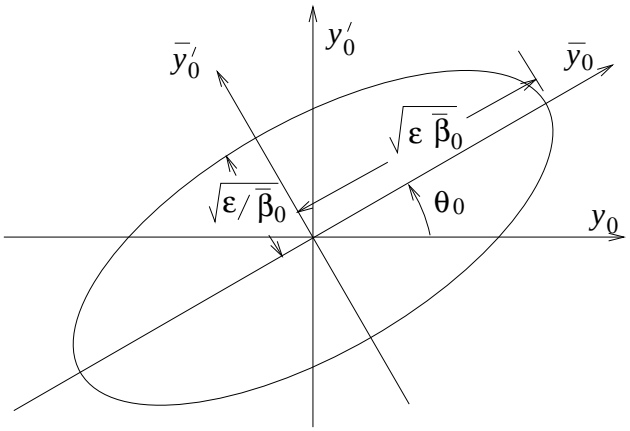

Figure 34: An elliptical beam in phase space. In the $(\overline{y}, \overline{y}')$-frame, skewed by angle θ_0, the ellipse is erect.

12.5 Elliptical (in phase space) beams

Because of the gigantic number of particles they contain, it is appropriate to represent entire beams by distribution functions. Beams that have elliptical shape in phase space are especially appropriate because, though the sizes, aspect ratios, and orientation vary with s, the shapes remain elliptical. The reason for this is that Eqs. (151) are linear. The sort of distribution envisaged is illustrated in Fig. 34.

for electron storage rings). When expressed in coordinates aligned with the ellipse, the general equation of the beam ellipse at $s = s_0$, as shown in Fig. 34, is

$$\frac{\overline{y}_0^2}{\overline{\beta}_0} + \overline{\beta}_0 \overline{y}_0'^2 \equiv \overline{\mathbf{y}}_0^T \begin{pmatrix} 1/\overline{\beta}_0 & 0 \\ 0 & \overline{\beta}_0 \end{pmatrix} \overline{\mathbf{y}} = \epsilon_y. \quad (165)$$

However the beam evolves, its outline has this equation, with appropriate parameters $\overline{\beta}(s), \theta(s), \epsilon_y$. The aspect ratio of the ellipse is governed by $\overline{\beta}(s)$ and its area is given

by

$$\boxed{\text{vertical phase space area} = \pi \sqrt{\epsilon_y \overline{\beta}}\, \sqrt{\epsilon_y / \overline{\beta}} = \pi \epsilon_y .} \tag{166}$$

Since this area has been previously shown to be invariant, the parameter ϵ_y is, in fact, *invariant*, which is why it has been given no subscript 0, nor overhead bar, nor argument s. ϵ_y is known as the beam "emittance"

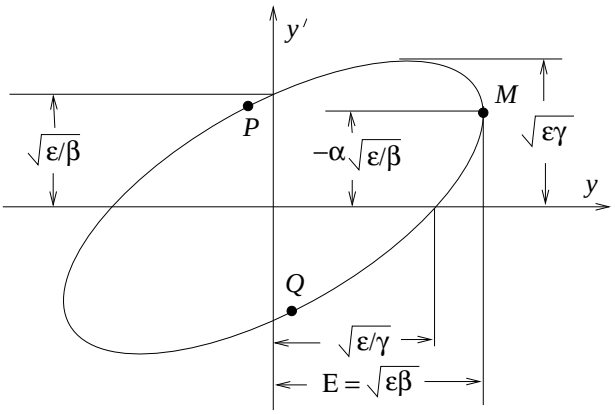

Figure 35: Correlating beam ellipse parameters with ellipse geometry.

$$\begin{pmatrix} \gamma_0 & \alpha_0 \\ \alpha_0 & \beta_0 \end{pmatrix} = \mathbf{R}_0^{-1} \begin{pmatrix} 1/\overline{\beta}_0 & 0 \\ 0 & \overline{\beta}_0 \end{pmatrix} \mathbf{R}_0 . \tag{169}$$

Since all factors on the right hand side have unit determinant, so also must the left hand side, and hence

$$\gamma_0 = \frac{1 + \alpha_0^2}{\beta_0} . \tag{170}$$

Using this relation and "completing squares", ellipse equation (168) can be simplified to

$$\frac{y_0^2 + (\alpha_0 y_0 + \beta_0 y_0')^2}{\beta_0} = \epsilon_y . \tag{171}$$

When ϵ_y is expressed in terms of the particle coordinates in this way it is known as the "Courant-Snyder" invariant; $\epsilon_{CS}(y, y')$. Note that the Courant-Snyder invariant is a property of a *particle* while emittance is a property of a *beam*—an unfortunate clash of the same symbol ϵ having different meanings.

12.6 Beam envelope $E(s)$

To interpret the meanings of the lattice functions β, α, and γ one can study the geometry of points on the beam ellipse, as shown in Fig. 35. Of greatest interest is the maximum (vertical in this case) excursion $E(s)$ of the ellipse, since this can be compared with a scraper position, or collimator size, to see whether the particle or ray will "wipe out". The abscissa of point M in Fig. 35 is given by

$$\boxed{E_y(s) = \sqrt{\epsilon_y \beta_y(s)}\,,} \tag{174}$$

The aperture "stay clear" must exceed $E_y(s)$ to avoid particle loss. It is because of the appearance of β in this formula that β is usually considered to be the most important Twiss beam parameter. It can be seen from Fig. 36 that the slope of the beam envelope at point M is the same as the slope of the particular ray defined by point M, which is given by $y'(M) = -\alpha_y \sqrt{\epsilon_y / \beta_y}$. Differentiating Eq. (174), this makes it possible to obtain the rate of change of the beam envelope;

$$E_y'(s) \equiv \frac{dE_y}{ds} = \frac{\beta_y'}{2} \sqrt{\frac{\epsilon_y}{\beta_y}} . \tag{175}$$

Equating y' to E_y' yields

$$\beta' = -2\alpha, \tag{176}$$

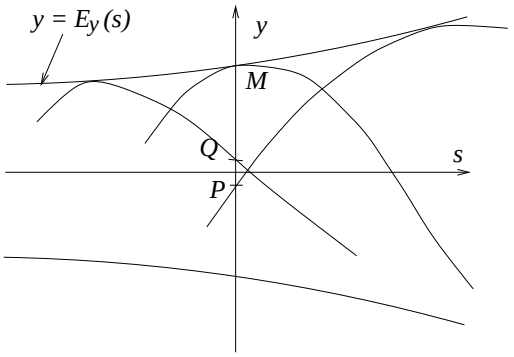

Figure 36: The beam envelope $E_y(s)$ is equal to the maximum transverse excursion y at longitudinal position s. Point labels M, P, and Q correspond approximately to Fig. 35.

12.8 **Pseudoharmonic trajectory description**

It has been seen in Eq. (174) that the beam envelope scales proportional to $\sqrt{\beta}$. One conjectures therefore, that individual trajectories will scale the same way and be describable in the form

$$\boxed{y(s) = a\sqrt{\beta(s)}\,\cos(\psi(s) - \psi_0),} \tag{184}$$

where ψ depends on s and a is a constant amplitude. This form has to satisfy Eq. (146), and the $\cos(\psi - \psi_0)$ "ansatz" is based on the known solution when $K(s)$ is, in fact, constant. This is the basis for naming the trajectory description "pseudoharmonic". As β appears in this equation, it has no apparent *beam* attribute and it will be referred to as a "lattice function". Differentiating Eq. (184) we get

$$y'(s) = -a\sqrt{\beta(s)}\,\psi'\,\sin(\psi - \psi_0) + \frac{a\beta'}{2\sqrt{\beta}}\,\cos(\psi - \psi_0). \tag{185}$$

Substituting into Eq. (146) we can demand that the coefficients of sin and cos terms vanish independently, since that is the only way of maintaining equality for all values of ψ_0. This leads to the equations

$$\begin{aligned} &\beta\,\psi'' + \beta'\psi' = 0, \\ &2\beta\,\beta'' - \beta'^2 - 4\beta^2\psi'^2 + 4\beta^2 K(s) = 0. \end{aligned} \tag{186}$$

From the first equation it follows that $\beta\psi'$ is constant. To obtain the conventional description we pick this constant to be 1 and obtain

$$\psi' = \frac{1}{\beta}, \quad \text{or} \quad \psi(s) = \psi(s_0) + \int_{s_0}^{s} \frac{ds'}{\beta(s')}. \tag{187}$$

Since ψ is the argument of a sinusoidal function, and the argument of a harmonic wave is $2\pi s/\text{wavelength}$, this permits us to interpret $2\pi\beta(s)$ as a "local wavelength" or, equivalently, $1/\beta(s)$ is the "local wave number". Substituting into the second of Eqs. (186), we obtain

$$\beta'' = 2\beta K(s) + 2\frac{1+\beta'^2/4}{\beta}. \tag{188}$$

This second order, nonlinear differential equation is usually considered to be the fundamental defining relationship for the evolution of the lattice β-function. Like any differential equation its solution is unique only if initial conditions or boundary conditions are given. The possiblilities are:

- Initial conditions β_0, β $(= -2\alpha_0)$ are given, for example at the beginning of a beam transfer line. A "matched transfer line" also has specified values, β_1, α_1, at its exit. (Satisfying these extra conditions requires the lens strengths in the line to be tuned appropriately.)
- Values are given at two points, β_0 and β_1. This is uncommon.
- The function $\beta(s)$ is required to be periodic with period C where C is the circumference of a storage ring (or the period of a periodic lattice); $\beta(0) = \beta(C)$, $\alpha(0) = \alpha(C)$. This is the most important case.

Because $K(s)$ depends on s, solving the equation may be quite difficult in general. An artist's conception of the β-function corresponding to a somewhat typical, stepwise-constant, focusing profile is exhibited in Fig. 37. The figure also shows a sine-like trajectory, which executes something like three quarters of a full oscillation in this section, so the "tune" is about 0.75. (A typical storage ring would be made up of some number n_c of cells like this so the circumference would be $n_c C_1$ and the tune would be about $0.75 n_c$.)

A "first integral" of Eq. (188) can be obtained by squaring and adding Eqs. (184) and (185) (rearranged) to give

$$\frac{y^2}{\beta} + \beta(y' - \frac{\beta'}{2\beta}y)^2 = a^2. \tag{189}$$

According to Eq. (176) we have $\beta' = -2\alpha$, so this result confirms the constancy of the Courant-Snyder invariant, (Eq. (171)), and a^2 can be identified with what was previously called $\epsilon_{y,b}$. There is an essential new feature however. In Eq. (171) the constancy referred to all points on the beam ellipse. Here it refers to all points s on a single ray or trajectory.

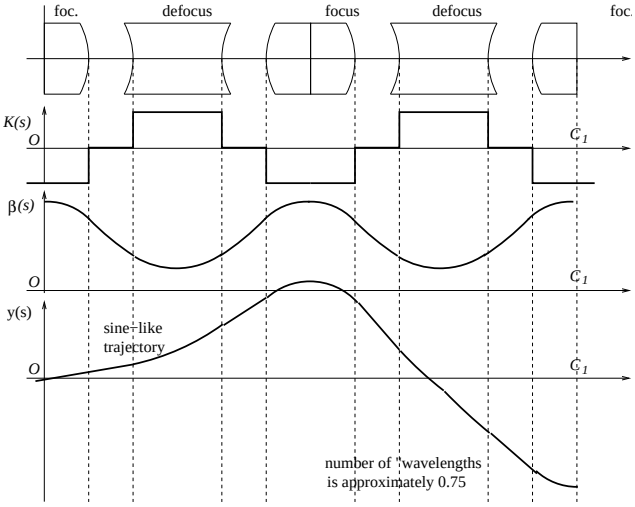

Figure 37: Pictorial representation of β-function variation corresponding to a possible focusing profile $K(s)$ produced, for example, by the long quadrupoles shown. The lower figure shows the sine-like trajectory. The "tune" of this section of beam line is about 0.75 since the trajectory goes through roughly 3/4 of a full wavelength.

```
Beta function is periodic.

Orbit is not periodic.


<--- periodic boundary conditions
```

IP optics

"Hourglass effect"

In light optics beta*
is the "Rayleigh length"

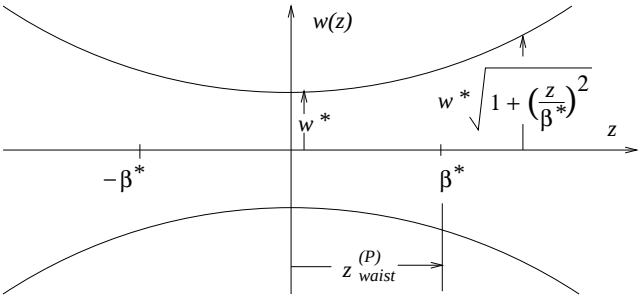

Figure 39: Longitudinal variation of beam half-width $w(z)$ near a beam waist.

Completing the multiplication, one finds

$$\begin{aligned} \beta &= \beta_0 - 2\alpha_0 s + \gamma_0 s^2, \\ \alpha &= \alpha_0 - \gamma_0 s, \\ \gamma &= \gamma_0. \end{aligned} \tag{194}$$

One finds, upon substituting $\beta(s)$ given here into lattice Eq. (188), that the beam-based $\beta(s)$ satisfies the lattice-based differential equation, If the two versions of β are equal at one point in the drift section, they will remain equal throughout the section.

Behavior of the lattice functions in the vicinity of a "beam waist" (traditionally signified by asterisk *) will be especially important. At such a point $\alpha \equiv \alpha^* = 0$, so $\beta = \beta^*$ has an extreme value, which we take to be a minimum. At a waist $\gamma^* = 1/\beta^*$. Eqs. (194) describes the evolution of β away from that point. To emphasize that the formula applies only in drift regions we will replace s by z. Substituting into the first of Eqs. (194) we obtain

$$\beta(z) = \beta^* + \frac{z^2}{\beta^*}. \tag{195}$$

A "waist length" can be defined by

$$z^{(P)}_{\rm waist} = \beta^*; \tag{196}$$

it is the length after which the beam transverse-dimension-squared has doubled.[19] [20] Because the transverse beam size is proportional to $\sqrt{\beta}$, the variation of the beam half-width is given by

$$E(z) = E^* \sqrt{1 + (z/\beta^*)^2}, \tag{197}$$

as shown in Fig. 39.

12.10 *Reconciliation of beam and lattice parameters*

Beam evolution through a drift section. Suppose the region from s_0 to s is purely a drift section. According to Eq. (155) and the first of Eqs. (172), the beam evolution is given by

$$\begin{matrix} \gamma & \alpha \\ \alpha & \beta \end{matrix} = \begin{matrix} 1 & 0 \\ s & 1 \end{matrix} \begin{matrix} \gamma_0 & \alpha_0 \\ \alpha_0 & \beta_0 \end{matrix} \begin{matrix} 1 & -s \\ 0 & 1 \end{matrix} \tag{193}$$

Beam evolution through a thin lens. Consider next the beam evolution in passing through a thin lens. According to Eq. (158) and the first of Eqs. (172), the beam evolution is given by

$$\begin{matrix} \gamma_+ & \alpha_+ \\ \alpha_+ & \beta_+ \end{matrix} = \begin{matrix} 1 & -q \\ 0 & 1 \end{matrix} \begin{matrix} \gamma_- & \alpha_- \\ \alpha & \beta \end{matrix} \begin{matrix} 1 & 0 \\ q & 1 \end{matrix} \tag{198}$$

Completing the multiplication, one finds

$$\begin{aligned}\beta_+ &= \beta_-,\\ \alpha_+ &= \alpha_- - \beta\, q,\\ \gamma_+ &= \gamma_- - 2\alpha_- q + \beta\, q^2.\end{aligned} \tag{199}$$

For lines made up only of drifts and thin lenses, it has therefore been shown that beam-based and lattice-based Twiss functions, if once equal, remain equal. Since, as stated earlier, all transfer matrices can be constructed from drifts and thin lenses, the result is true for any general (uncoupled) beam line.

Parameter	Symbol	Proportionality	Scaling
phase advance per cell	μ		1
collider cell length	L_c		$R^{1/2}$
bend angle per cell	ϕ	$= L_c/R$	$R^{-1/2}$
quad strength $(1/f)$	q	$1/L_c$	$R^{-1/2}$
dispersion	D	ϕL_c	1
beta	β	L_c	$R^{1/2}$
tunes	Q_x, Q_y	R/β	$R^{1/2}$
Sands's "curly H"	$\mathcal{H}$	$= D^2/\beta$	$R^{-1/2}$
partition numbers	$J_x/J_y/J_\epsilon$	$= 1/1/2$	1
horizontal emittance	ϵ_x	$\mathcal{H}/(J_x R)$	$R^{-3/2}$
fract. momentum spread	σ_δ	$\sqrt{B}$	$R^{-1/2}$
arc beam width-betatron	$\sigma_{x,\beta}$	$\sqrt{\beta\epsilon_x}$	$R^{-1/2}$
-synchrotron	$\sigma_{x,synch.}$	$D\sigma_\delta$	$R^{-1/2}$
sextupole strength	S	q/D	$R^{-1/2}$
dynamic aperture	$x^{\max}$	q/S	1
relative dyn. aperture	$x^{\max}/\sigma_x$		$R^{1/2}$
pretzel amplitude	x_p	σ_x	$R^{-1/2}$

Parameter	Symbol	Value	Unit	Energy-scaled	Radius-	scaled
bend radius	R	**3026**	m	**3026**	**5675**	**11350**
	$R/3026$			1	1.875	3.751
Beam Energy	E	**45.6**/91.5	GeV	**120**	**120**	**120**
Circumference	C	26.66	km	26.66	50	100
Cell length	L_c		m	79	108	153
Momentum compaction	α_c	1.85e-4		1.85e-4	0.99e-4	0.49e-4
Tunes	Q_x	90.26		90.26	123.26	174.26
	Q_y	76.19		76.19	104.19	147.19
Partition numbers	$J_x/J_y/J_\epsilon$	1/1/2		1/1.6/1.4 !	1/1/2	1/1/2
Main bend field	B_0	0.05/0.101	T	0.1316	0.0702	0.0351
Energy loss per turn	U_0	0.134/2.05	GeV	6.49	3.46	1.73
Radial damping time	τ_x	0.06/0.005	s	0.0033	0.0061	0.0124
	τ_x/T_0	679/56	turns	37	69	139
Fractional energy spread	σ_δ	0.946e-3/1.72e-3		0.0025	0.0018	0.0013
Emittances (no BB), x	ϵ_x	22.5/30	nm	21.1	8.2	2.9
y	ϵ_y	0.29/0.26	nm	1.0	0.4	0.14
Max. arc beta functs	$\beta_x^{\max}$	125	m	125	171	242
Max. arc dispersion	$D^{\max}$	0.5	m	0.5	0.5	0.5
Beta functions at IP	β_x^*, β_y^*	2.0,0.05	m	1.25/0.04	N/Sc.	N/Sc.
Beam sizes at IP	σ_x^*, σ_y^*	211, 3.8	μm	178/11	N/Sc.	N/Sc.
Beam-beam parameters	ξ_x, ξ_y	0.037,0.042		0.06/0.083	N/Sc.	N/Sc.
Number of bunches	N_b	8		4	N/Sc.	N/Sc.
Luminosity	$\mathcal{L}$	2e31	$\mathrm{cm}^{-2}\mathrm{s}^{-1}$	1.0e32	N/Sc.	N/Sc.
Peak RF voltage	V_{RF}	380	MV	3500	N/Sc.	N/Sc.
Synchrotron tune	Q_s	0.085/0.107		0.15	N/Sc.	N/Sc.
Low curr. bunch length	σ_z	0.88	cm	$\frac{\alpha_c R \sigma_e}{Q_s E}$	N/Sc.	N/Sc.

Table 5: Higgs factory parameter values for 50 km and 100 km options. The entries are mainly extrapolated from Jowett's, 45.6 Gev report [8], and educated guesses. "N/Sc." indicates (important) parameters too complicated to be estimated by scaling. Duplicate entries in the third column, such as 45.6/91.5 are from Jowett [8]; subsequent scalings are based on the 45.6 Gev values.